Fractional spin and Josephson effect in time-reversal-invariant topological superconductors

Alberto Camjayi,[1] Liliana Arrachea,[2] Armando Aligia,[3] and Felix von Oppen[4]

[1] *Departamento de Física, FCEyN, Universidad de Buenos Aires and IFIBA, Pabellón I, Ciudad Universitaria, 1428 CABA Argentina*
[2] *International Center for Advanced Studies, ECyT-UNSAM, Campus Miguelete, 25 de Mayo y Francia, 1650 Buenos Aires, Argentina*
[3] *Centro Atómico Bariloche and Instituto Balseiro, CNEA, 8400 S. C. de Bariloche, Argentina*
[4] *Dahlem Center for Complex Quantum Systems and Fachbereich Physik, Freie Universität Berlin, 14195 Berlin, Germany*

Time reversal invariant topological superconducting (TRITOPS) wires are known to host a fractional spin $\hbar/4$ at their ends. We investigate how this fractional spin affects the Josephson current in a TRITOPS-quantum dot-TRITOPS Josephson junction, describing the wire in a model which can be tuned between a topological and a nontopological phase. We compute the equilibrium Josephson current of the full model by continuous-time Monte Carlo simulations and interpret the results within an effective low-energy theory. We show that in the topological phase, the 0-to-π transition is quenched via formation of a spin singlet from the quantum dot spin and the fractional spins associated with the two adjacent topological superconductors.

PACS numbers: 74.78.Na, 74.45.+c, 73.21.La

Introduction.—The interplay of many-body interactions in quantum dots and superconductivity has been at the focus of interest for some time [1–6]. While electrons are paired in superconductors, the charging energy effectively suppresses pairing in quantum dots. A prominent consequence of this competition is the transition between 0 and π junction behavior of the Josephson current in devices where a quantum dot (QD) connects between ordinary (nontopological) singlet-superconducting wires (S-QD-S junction) [7–10]. As a result of numerous studies [11–18], this phenomenon is now well understood for conventional superconductors. Essentially, S-QD-S junctions exhibit π-junction behavior when the QD hosts an effective spin-1/2 degree of freedom.

Here, we address the 0 to π transition for Josephson junctions in which a quantum dot connects between time-reversal-invariant topological superconductors (TRITOPS). Unlike their time-reversal-breaking cousins [19–22], TRITOPS preserve time-reversal symmetry and can coexist with an unpolarized quantum-dot spin. It is thus an interesting question whether π-junction behavior can be observed in TRITOPS-QD-TRITOPS junctions. Such junctions differ from conventional S-QD-S junctions in several ways. First, the Majorana-Kramers pairs present in the topological phase allow for the coherent transfer of single electrons, while the Josephson current of a conventional junction is carried by Cooper pairs. Even more intriguing, TRITOPS host a fractional $\hbar/4$ spin at their ends. Thus, a TRITOPS-QD-TRITOPS junction allows one to study the hybridization of fractional and ordinary spins. We show that the 0-π transition constitutes a signature which distinguishes between the topological and the nontopological phase, and trace the quenching of the transition for TRITOPS to the formation of a spin singlet from the quantum-dot spin and the fractional spins of the adjacent TRITOPS.

In the wake of proposals to engineer time-reversal-breaking topological phases and corresponding experiments, there has also been substantial interest in time reversal invariant topological superconductors (TRIPTOPS) [23–35]. TRITOPS are characterized by Kramers pairs of Majorana end states and localized fractional spins [27]. Time reversal protects the pair of Majoranas from hybridizing which therefore generically remain at zero energy. Similarly, the fractional spin is topologically protected and cannot be determined from a local measurement without breaking time reversal. Several routes have been proposed to engineer TRITOPS although their experimental realization is more demanding than that of time-reversal-breaking topological superconductors [35].

Conventional Josephson junctions assume their minimal energy at zero phase difference and their maximal energy at a phase difference of π (0-junction behavior). This behavior is reversed in π junctions which assume their minimal energy at a phase difference of π [1, 2]. In S-QD-S junctions, π-junction behavior occurs when the quantum dot forming the junction is singly occupied and acts effectively as a magnetic impurity. When the QD is weakly coupled to the superconductors, tunneling of Cooper pairs between the conventional superconductors relies on a forth-order cotunneling process [1, 10]. This process includes a π phase shift which originates from the Fermi statistics of electrons and becomes manifest in the π-junction behavior. As a consequence, the current-phase relation of the junction phase shifts by π when the occupation of the quantum dot is tuned from even to odd. When the quantum dot is strongly coupled to the superconductors, Kondo correlations become relevant. For a sufficiently large Kondo temperature T_K, the dot spin

is Kondo screened and the junction exhibits 0-junction behavior even when the dot occupation is odd.

Model.—Our considerations are based on a time-reversal-invariant superconductor with Hamiltonian [26]

$$H_\alpha = \sum_{j=1}^{N}\sum_{\sigma}\Big(-tc^\dagger_{\alpha,j+1,\sigma}c_{\alpha,j,\sigma} + i\lambda_\sigma c^\dagger_{\alpha,j+1,\sigma}c_{\alpha,j,\sigma} + \Delta_\sigma e^{i\phi_\alpha}c^\dagger_{\alpha,j+1,\sigma}c^\dagger_{\alpha,j,\overline{\sigma}} + \text{H.c.} - \mu\, n_{\alpha,j,\sigma}\Big), \quad (1)$$

where $\lambda_{\uparrow,\downarrow} = \pm\lambda$, $\Delta_{\uparrow,\downarrow} = \pm\Delta$ and $\overline{\uparrow} = \downarrow$, $\overline{\downarrow} = \uparrow$. Moreover, t is the hopping parameter, μ the chemical potential, and λ and Δ are the strengths of Rashba spin-orbit coupling and extended s-wave pairing, respectively. The index $\alpha = L, R$ labels the left and right superconductors of the junction with order parameter phases ϕ_α. The phase difference $\phi = \phi_L - \phi_R = 2\pi\Phi/\Phi_0$ can be tuned by including the junction in a superconducting loop and threading the loop by a magnetic flux Φ. ($\Phi_0 = h/2e$ denotes the superconducting flux quantum.) The entire TRITOPS-QD-TRITOPS Josephson junction is then described by the Hamiltonian

$$H = \sum_{\alpha=L,R} H_\alpha + H_c + H_d. \quad (2)$$

Here,

$$H_d = \varepsilon_d \sum_\sigma n_{d,\sigma} + U n_{d\uparrow} n_{d\downarrow} \quad (3)$$

describes the quantum dot with gate-tunable level energy ε_d, spin-resolved level occupation $n_{d,\sigma}$, and charging energy U, and

$$H_c = -t' \sum_\sigma \left[\left(c^\dagger_{L,N,\sigma} + c^\dagger_{R,1,\sigma}\right) d_\sigma + \text{H.c.}\right] \quad (4)$$

accounts for the hybridization between quantum dot and superconductors.

The Hamiltonian H_α supports topological and nontopological phases. The topological phase occurs when $|\mu| < 2\lambda$ and is characterized by Kramers pairs of Majorana end states. For each lead, the corresponding Majorana operators can be combined into conventional fermionic operators

$$\gamma_{L/R} = \int \mathrm{d}x \varphi_{L/R}(x)[\psi_\uparrow(x) \mp i\psi^\dagger_\downarrow(x)], \quad (5)$$

where $\varphi_{L/R}(x)$ denotes the Majorana wavefunctions of the left (L) and right (R) superconducting lead and $\psi_\sigma(x)$ denotes the electron field operator for spin σ (see Supplementary Material, Sec. 2 [36]). While the Majorana operators mix the two spin components, the operators $\gamma_{L/R}$ remove a spin of $\hbar/2$ from one end of the wire. Thus, $\gamma_{L/R}$ and $\gamma^\dagger_{L/R}$ toggle the the system between ground states with fractional spins of $\pm\hbar/4$ localized at the ends of the wire [27].

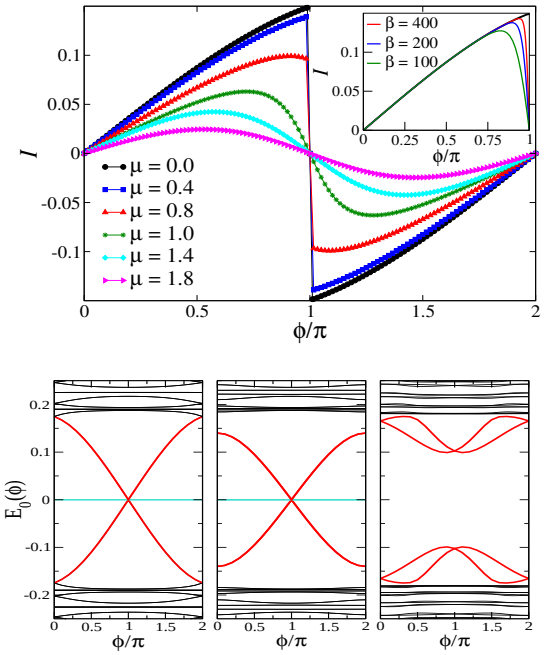

FIG. 1. (Color online) Top: Josephson current *vs* ϕ for a quantum dot at $T = 0$ with $U = 0$, $t' = t$, $\lambda = t/2$, $\Delta = t/5$, and values of μ in the topological ($\mu < t$) as well as the nontopological ($\mu > t$) phase. The wires have $N = 500$ sites. Inset: Josephson current at finite temperature. Red, blue, and green lines correspond to $\beta = 400, 200$ and 100, respectively. The $T = 0$ case is plotted in black for reference. Bottom: Spectrum of $\hat{\mathcal{H}}_{BdG}$ for $\mu = \varepsilon_d = 0$ (left), $\mu = 0$, $\varepsilon_d = t$ (middle), and $\mu = -\varepsilon_d = 1.8$ (right). Other parameters as in top panel. Energies are measured in units of $t = 1$.

Numerical results.—The Josephson current can be computed from the Green function expression

$$I = \frac{2t'^2}{\beta}\sum_\sigma\sum_n \mathrm{Im}\left[g^{(12)}_{1\alpha,\sigma}(i\omega_n)G^{(21)}_{d,\sigma}(i\omega_n)\right]. \quad (6)$$

The derivation is included in Ref. [36] (see Sec. 1). The Green functions correspond to the Matsubara components of frequency $\omega_n = (2n+1)\pi/\beta$ (β is the inverse temperature) of the imaginary-time Green functions $g^{(12)}_{1\alpha,\sigma}(\tau) = -\langle T_\tau\left[\hat{c}^\dagger_{\alpha,1,\sigma}(\tau)\hat{c}^\dagger_{\alpha,1,\overline{\sigma}}(0)\right]\rangle_0$ and $G^{(21)}_{d,\sigma}(\tau) = -\langle T_\tau\left[\hat{d}_\sigma(\tau)\hat{d}_{\overline{\sigma}}(0)\right]\rangle$, where $\langle\ldots\rangle_0$ ($\langle\ldots\rangle$) denotes the ensemble average over the states of H_α (H). The first Green function can be obtained exactly.

First consider a junction with a noninteracting quantum dot. For $U = 0$, the Green function $G_{d,\sigma}(i\omega_n)$ and thus the Josephson current can also be evaluated analytically. Moreover, our model can be written in Nambu representation with a Bogoliubov de-Gennes (BdG) Hamiltonian $\hat{\mathcal{H}}_{BdG} = \hat{\mathcal{H}}_0\tau_z + \hat{\Delta}\tau_x$, where $\hat{\mathcal{H}}_0$ results from the normal parts of the Hamiltonian H while $\hat{\Delta}$ originates from the pairing contributions. The Pauli matrices τ_i

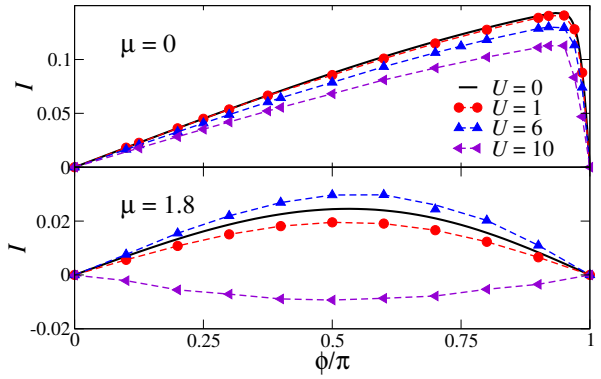

FIG. 2. (Color online) Josephson current for an interacting quantum dot at $\beta = 400$ with $t' = t$, $\varepsilon_d = -U/2$, $\lambda = t/2$, $\Delta = t/5$. The upper (lower) panel corresponds to the topological (nontopological) phase. The values of U and μ are indicated in the Fig. Energies are expressed in units of $t = 1$.

(with $i = x, y, z$) operate in particle-hole space. Diagonalizing the BdG Hamiltonian, the Josephson current can be obtained from $I = (2e/\hbar)\partial E_0(\phi)/\partial\phi$, where $E_0(\phi)$ is the many-body ground state energy. Corresponding results are presented in Fig. 1.

The spectrum of $\hat{\mathcal{H}}_{BdG}$ is shown in the lower panels for the topological (left and middle) and the nontopological (right) phase. In the topological phase, there are zero-energy bound states (light-blue curves) which emerge from the Majoranas states localized at the far ends of the finite-length chains. The solid red curves emerge from the hybridization of the dot states with the adjacent Majoranas. In the nontopological phase, the subgap states are gapped. As a consequence of Kramers theorem, the subgap states are twofold degenerate at ϕ equal to integer multiples of π. At other flux values, time reversal is broken by the phase bias and the subgap states are nondegenerate. The top panel of Fig. 1 shows the Josephson current for values of μ both in the topological ($\mu < 2\lambda$) and the nontopological ($\mu > 2\lambda$) phases. In the topological phase, the Josephson current jumps at $\phi = \pi$ (up to finite-size effects), reflecting the level crossing of the subgap states. (Note that we assume complete equilibration over fermion parities.) The nontopological phase exhibits the usual smooth behavior.

For a nonzero interaction U, the Josephson current can be calculated by evaluating $G^{(21)}_{d,\sigma}(i\omega_n)$ using quantum Monte Carlo simulations [37]. Previous works on S-QD-S junctions [12, 15, 16] as well as normal wires coupled to correlated dots and molecules [38, 39] proved this strategy to be accurate and reliable. We perform a Shiba transformation, mapping H to a particle-number conserving Hamiltonian with negative U [15]. The Green function of the transformed problem is then calculated by the algorithm introduced in Refs. [40, 41]. Inversion of the Shiba transformation leads to $G_{d,\sigma}(i\omega_n)$ which enters the Josephson current (6). Results for a half-filled configuration (i.e., $\langle n_{d\uparrow} + n_{d\downarrow}\rangle = 1$) are shown in Fig. 2.

The nontopological case (bottom panel) shows the expected 0 to π transition. When coupling the quantum dot to superconducting leads, the local moment persists when Δ is larger than the Kondo temperature T_K, but becomes Kondo screened for $\Delta \ll T_K$. For a particle-hole symmetric configuration, the Kondo temperature of the junction is given by $k_B T_K = \sqrt{\Gamma U/2}\exp(-\pi U/8\Gamma)$ [42] with the hybridization parameter $\Gamma \sim \pi(t')^2\sqrt{1-\mu^2/(2t)^2}/(2t)$. Consequently, there is a 0-π transition as U increases. For $U = t$, the dot is in the intermediate valence regime, while for $U = 6t$ and $U = 10t$, it would be in the Kondo regime when attached to normal leads. In our case, $k_B T_K \sim \Delta$ for $U \sim 8.5t$, consistent with the observed transition between 0- and π-junction behavior between $U = 6t$ and $U = 10t$.

It is our central observation that there is no corresponding 0-π transition when the superconducting leads are in the topological regime. Instead, the current-phase relation remains similar to the noninteracting case for all interaction strengths U. In particular, the abrupt dependence at a phase difference of $\phi = \pi$, while slightly smoothed by finite temperature, becomes more pronounced as the number of sites increases, as in the noninteracting case (cp. inset of Fig. 1). These results suggest that the impurity spin is efficiently screened in the topological case, despite the presence of the superconducting gap. This robust screening of the spin of the quantum dot originates from its interaction with the subgap states emerging from the Kramers pairs of Majoranas of the adjacent left and right wires.

Effective Hamiltonian.—To arrive at this conclusion, we interpret our numerical results in the context of an effective Hamiltonian. Consider a singly-occupied, interacting quantum dot coupled to two time-reversal-invariant topological superconductors. For simplicity, we assume that the superconducting gap is large compared to the Kondo temperature so that we can neglect hybridization with the quasiparticle continuum. Then, we only need to consider the hybridization with the subgap states originating from the Majorana bound states. We can project out the empty and doubly occupied dot states by employing a Schrieffer-Wolff transformation [43]. This yields an effective Hamiltonian in the eight-dimensional subspace spanned by the two eigenstates of the quantum dot spin $\mathbf{S}_d$ and the two states for each of the superconducting leads which are associated with the Kramers pair of Majorana operators. Here, we sketch the derivation of this Hamiltonian (for details, see [36], Sec. 3).

In a first step, we project the tunneling Hamiltonian H_c to the subgap states of the wires, giving $H_c = t_{\rm eff} e^{i\phi/4}\sum_\sigma \left(\gamma^\dagger_{L,\sigma} d_\sigma + d^\dagger_\sigma \gamma_{R,\sigma}\right) + \text{H.c}$, where $t_{\rm eff} \lesssim t'$ and the Bogoliubov operators for the zero-energy modes sat-

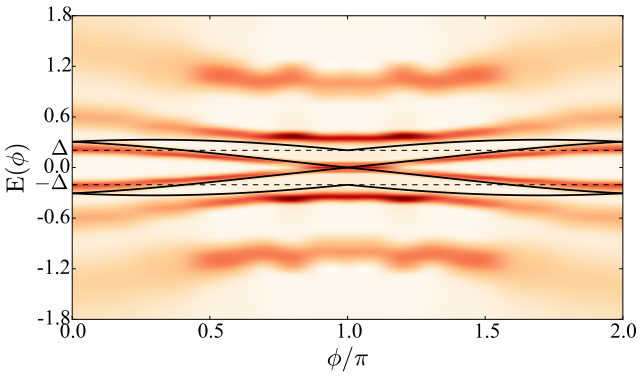

FIG. 3. (Color online) LDOS at the quantum dot obtained by QMC. The black lines are the predictions for the peaks in the density of states on the basis of $H_{\rm eff}$ with $J = 0.2$. The amplitude of the superconducting gap $\Delta = 0.2$ is indicated in dashed lines. Other parameters are $U = 4t$, $J = 0.2$, $\lambda = 0.5t$, $t' = t$, $\mu = 0$ and $\beta = 400$.

isfy $\gamma_L^\dagger = \gamma_{L,\uparrow}^\dagger = i\gamma_{L,\downarrow}$, and $\gamma_R^\dagger = \gamma_{R,\uparrow}^\dagger = -i\gamma_{R,\downarrow}$ (see [44] and [36], Sec. 2). Focusing on the particle-hole symmetric point $\varepsilon_d = -U/2$, and eliminating the empty and doubly occupied states of the quantum dot by a Schrieffer-Wolff transformation, we obtain (see [36], Sec. 3)

$$H_{\rm eff} = J\left\{S_d^z\left[(n_L+n_R-1) + i\sin\frac{\phi}{2}\left(\gamma_L^\dagger\gamma_R - \gamma_R^\dagger\gamma_L\right)\right] + i\cos\frac{\phi}{2}\left(S_d^-\gamma_L^\dagger\gamma_R^\dagger - S_d^+\gamma_R\gamma_L\right)\right\}, \quad (7)$$

where $J = 4t_{\rm eff}^2/U$ and we defined the occupations $n_\alpha = \gamma_\alpha^\dagger\gamma_\alpha$. A convenient basis for this Hamiltonian is $|\sigma, n_L, n_R\rangle$ with $n_\alpha = 0, 1$ and $\sigma = \uparrow, \downarrow$. Note that n_α also labels the polarization of the fractional spins.

The Hamiltonian $H_{\rm eff}$ is easily diagonalized. It conserves the number parity of $n = n_L + n_R$. For $n = 1$, the terms involving $S_d^\pm$ do not contribute and we find doubly-degenerate eigenstates which are linear superpositions of $|\sigma, 1, 0\rangle$ and $|\sigma, 0, 1\rangle$ with energy $\pm J/2\sin(\phi/2)$. For even occupations n, we have two phase-independent states with degenerate eigenergies $J/2$ corresponding to $|\uparrow, 1, 1\rangle$ and $|\downarrow, 0, 0\rangle$ as well as a pair of nondegenerate states with energies $-J/2 \pm J\cos(\phi/2)$, which are linear combinations of the states $|\uparrow, 0, 0\rangle$ and $|\downarrow, 1, 1\rangle$.

At all phase differences, the ground state is an equal-probability superposition of $|\uparrow, 0, 0\rangle$ and $|\downarrow, 1, 1\rangle$. These states describe configurations with overall zero spin. Indeed, in both states the quantum dot spin of $\hbar/2$ is pointing opposite to the fractional spins of $\hbar/4$ of the two adjacent superconductors. Thus, these configurations can be interpreted as an effective singlet configuration of the quantum dot spin and the fractional spins of the topological superconductors.

Similar to the singlet formation via the Kondo effect originating from the hybridization with the continuum state of nontopological superconductors, this singlet formation with the fractional spins quenches the π-junction behavior. Indeed, the low-energy spectrum emerging from the Schrieffer-Wolff treatment predicts a Josephson energy which is minimal at phase differences equal to integer multiples of 2π. Moreover, we also see that there is a cusp in the ground state energy at a phase difference of π. Both of these results are consistent with our numerical results which incorporate the hybridization with the quasiparticle continuum above the superconducting gap.

In Fig. 3, we benchmark our low-energy Hamiltonian with results for the local density of states (LDOS) at the quantum dot $\rho(\omega) = -2\sum_\sigma {\rm Im}[G_{d,\sigma}^R(\omega)]$. The latter was calculated by analytically continuing the Monte Carlo data to the real frequency axis. Results are shown in the color plot. The low-energy spectrum obtained from $H_{\rm eff}$ is shown as solid lines for comparison. The peaks in the LDOS reflect the energy necessary to add or remove one particle. Thus, the peak positions can be estimated from $H_{\rm eff}$ by the energy difference between the odd-parity eigenstates and the ground state, which yields $\pm[J/2 + J|\cos(\phi/2)| \pm J/2\sin(\phi/2)]$. We find that our numerics is qualitatively consistent with the predictions of $H_{\rm eff}$, although the numerics is performed in a regime where the addition spectrum already hybridizes with the quasiparticle continuum. Apart from shifts in energy, the hybridization lifts the degeneracies at $\phi = 0$ and 2π. Besides the low energy features which are qualitatively described by $H_{\rm eff}$, the numerical results also exhibit high-energy features at $\pm U/2$, which are associated with the charge-transfer peaks of the impurity Anderson model.

TRITOPS-QD-TRITOPS Josephson junctions combine topological superconductivity with time reversal symmetry and electron-electron interactions. This is similar to quantum spin Hall Josephson junctions including interactions either within the edge states [45, 46] or through coupling to an interacting quantum dot [47, 48]. These quantum spin Hall Josephson junctions exhibit an 8π-perodic Josephson effect which can be interpreted as resulting from the tunneling of $e/2$ charges enabled by the formation of Z_4 parafermions. While the system considered here shares some basic ingredients, its Josephson effect is 4π periodic. In addition to spin conservation, the present system differs in that it does not exhibit a fermion parity anomaly and the resulting spin transmutation discussed in Ref. [47].

Acknowledgements. We acknowledge support from CONICET, and UBACyT, Argentina as well as Deutsche Forschungsgemeinschaft and Alexander von Humboldt Foundation, Germany. LA thanks the ICTP-Trieste for hospitality through a Simons associateship. This work was sponsored by PIP 112-201101-00832 of CONICET and PICT 2013-1045, PICT 2012- of the ANPCyT.

[1] S. De Franceschi, L. Kouwenhoven, C. Schönenberger and W. Wersdorfer, Nature Nanotechology, **5**, 703 (2010).

[2] A. Martín-Rodero and A. Levy Yeyati, Adv. Phys. **60**, 899 (2011).

[3] M. R. Buitelaar, T. Nussbaumer, and C. Schönenberger, Phys. Rev. Lett. **89**, 256801 (2002).

[4] T. Sand-Jespersen, J. Paaske, B. M. Andersen, K. Grove-Rasmussen, H. I. Jorgensen, M. Aagesen, C. B. Sorensen, P. E. Lindelof, K. Flensberg, and J. Nygärd, Phys. Rev. Lett. **99**, 126603 (2007).

[5] C. Buizert, A. Oiwa, K. Shibata, K. Hirakawa, and S. Tarucha, Phys. Rev. Lett. **99**, 136806 (2007).

[6] J.-D. Pillet, P. Joyez, R. Žitko, and M. F. Goffman, Phys. Rev. B **88**, 045101 (2013).

[7] I.O. Kulik, Zh. Eksp. Teor. Fiz. **49**, 585 (1965) [Sov. Phys. JETP **22**, 841 (1966)].

[8] H. Shiba and T. Soda, Prog. Theor. Phys. **41**, 25 (1969).

[9] L. I. Glazman and K. A. Matveev, Pisma Zh. Eksp. Teor. Fiz. **49**, 570 (1989) [JETP Lett. **49**, 659 (1989)].

[10] B. I. Spivak and S. A. Kivelson, Phys. Rev. B **43**, 3740 (1991).

[11] E. Vecino, A. Martin-Rodero, and A. Levy Yeyati, Phys. Rev. B **68**, 035105 (2003).

[12] F. Siano and R. Egger , Phys. Rev. Lett. **93**, 047002 (2004).

[13] M.-S. Chi, M. Lee, K. Kang, and W. Belzig, Phys. Rev. B (R) **70**, 020502 (2004).

[14] T. Meng, P. Simon, S. Florens, Phys. Rev. B **79**, 224521 (2009).

[15] D. J. Luitz and F. F. Assaad, Phys. Rev. B **81**, 024509 (2010).

[16] D. J. Luitz, F. F. Assaad, T. Novotny, C. Karrasch, and V. Meden, Phys. Rev. Lett. **108**, 227001 (2012).

[17] A. Oguri, Y. Tanaka, and J. Bauer, Phys. Rev. B **87**, 075432 (2013).

[18] R. Allub and C. R. Proetto, Phys. Rev. B **91**, 045442 (2015).

[19] J. Alicea, Rep. Prog. Phys. **75**, 076501, (2012).

[20] A. Y. Kitaev, Physics-Uspekhi **44**, 131 (2001).

[21] R. M. Lutchyn, J. D. Sau,and S. Das Sarma, Phys. Rev. Lett. **105** 077001 (2010).

[22] Y. Oreg, G. Refael, and F. von Oppen, Phys. Rev. Lett. **105** 177002 (2010).

[23] C. L. M. Wong and K. T. Law, Phys. Rev. B **86**, 184516 (2012).

[24] S. Nakosai, Y. Tanaka, and N. Nagaosa, Phys. Rev. Lett. **108**, 147003 (2012).

[25] S. Deng, L. Viola and G. Ortiz, Phys. Rev. Lett. **108**, 036803 (2012).

[26] F. Zhang, C. L. Kane, and E. J. Mele, Phys. Rev. Lett. **111**, 056402 (2013).

[27] A. Keselman, L. Fu, A. Stern, and E. Berg, Phys. Rev. Lett. **111**, 116402 (2013).

[28] E. Dumitrescu and S. Tewari, Phys. Rev. B **88**, 220505 (2013).

[29] S. B. Chung, J. Horowitz, and X-L. Qi, Phys. Rev. B **88**, 214514 (2013).

[30] S. Nakosai, J. C. Budich, Y. Tanaka, B. Trauzettel, and N. Nagaosa, Phys. Rev. Lett. **110**, 117002 (2013).

[31] A. Haim, A. Keselman, E. Berg, and Y. Oreg, Phys. Rev. B **89**, 220504(R) (2014).

[32] E. Gaidamauskas, J. Paaske, and K. Flensberg, Phys. Rev. Lett. **112**, 126402 (2014).

[33] J. Klinovaja, A. Yacoby, and D. Loss, Phys. Rev. B **90**, 155447 (2014).

[34] C. Schrade, A. A. Zyuzin, J. Klinovaja, and D. Loss, Phys. Rev. Lett. **115**, 237001 (2015).

[35] A. Haim, E. Berg, K. Flensberg, and Y. Oreg, Phys. Rev. B **94**, 161110(R) (2016).

[36] Supplementary Material

[37] J.E. Hirsch and R. M. Fye, Phys. Rev. Lett. **56**, 2521 (1986).

[38] L. Arrachea and M. J. Rozenberg, Phys. Rev. B **72**, 041301 (2005).

[39] A. Camjayi and L. Arrachea, Phys. Rev. B **86**, 235143 (2012) and J. Phys.: Condens. Matter **26** 035602 (2014).

[40] P. Werner, A. Comanac, L. De Medici, M. Troyer, and A.J. Millis, Phys. Rev. Lett. **97**, 076405 (2006).

[41] K. Haule, Phys. Rev. B **75**, 155113 (2007).

[42] A. Hewson, *The Kondo Problem to Heavy Fermions*, Cambridge University Press (Cambridge, 1993).

[43] J. R. Schrieffer and P. A. Wolff, Phys. Rev. **149**, 491 (1966).

[44] We introduce the notation $\gamma_{L/R,\sigma}$ to make the tunneling Hamiltonian more compact. It also turns out that this notation is helpful in performing the Schrieffer-Wolff transformation (see [36], Section 3).

[45] F. Zhang and C.L. Kane, Phys. Rev. Lett. **113**, 036401 (2014).

[46] C. P. Orth, R. P. Tiwari, T. Meng, and T. L. Schmidt, Phys. Rev. B **91**, 081406(R) (2015).

[47] Y. Peng, Y. Vinkler-Aviv, P.W.Brouwer, L.I. Glazman, and F. von Oppen, arXiv:1609.01896 (2016).

[48] H.-Y. Hui and J.D. Sau, arXiv:1609.02909 (2016).